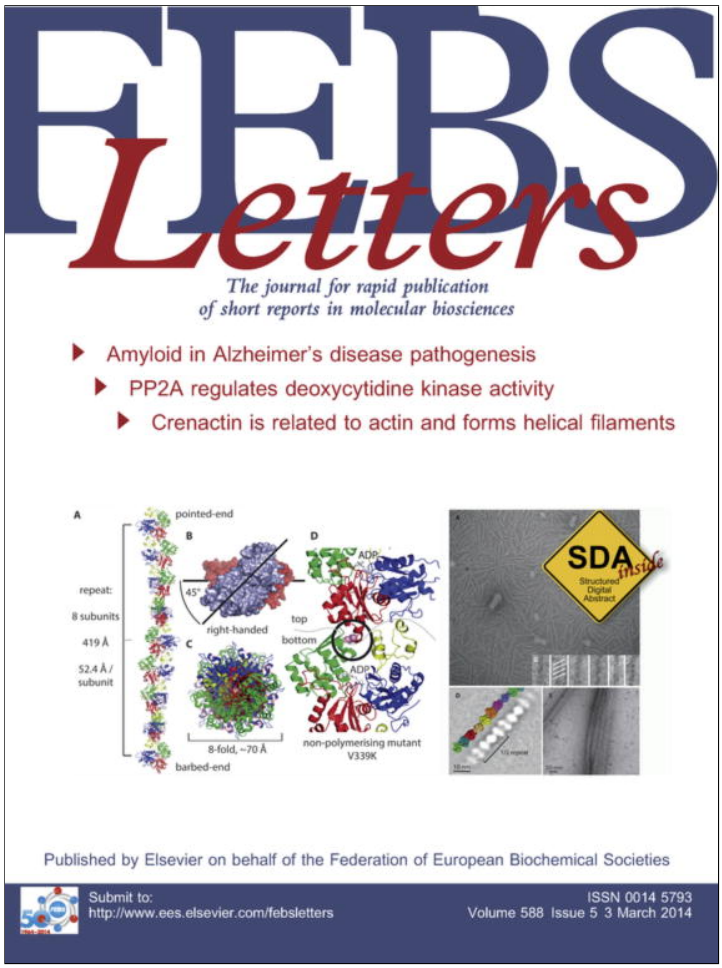

FEBS Letters 588 (2014) 836–844

journal homepage: www.FEBSLetters.org

EGF induces efficient Cx43 gap junction endocytosis in mouse embryonic stem cell colonies via phosphorylation of Ser262, Ser279/282, and Ser368

John T. Fong [1], Wutigri Nimlamool, Matthias M. Falk *

Department of Biological Sciences, Lehigh University, 111 Research Drive, Iacocca Hall, Bethlehem, PA 18015, USA

ARTICLE INFO

Article history:
Received 18 September 2013
Revised 15 January 2014
Accepted 16 January 2014
Available online 31 January 2014

Edited by Beat Imhof

Keywords:
Connexin43
Cx43 phosphorylation
Epidermal growth factor
Gap junction internalization
Mouse embryonic stem cells

ABSTRACT

Gap junctions (GJs) traverse apposing membranes of neighboring cells to mediate intercellular communication by passive diffusion of signaling molecules. We have shown previously that cells endocytose GJs utilizing the clathrin machinery. Endocytosis generates cytoplasmic double-membrane vesicles termed annular gap junctions or connexosomes. However, the signaling pathways and protein modifications that trigger GJ endocytosis are largely unknown. Treating mouse embryonic stem cell colonies – endogenously expressing the GJ protein connexin43 (Cx43) – with epidermal growth factor (EGF) inhibited intercellular communication by 64% and activated both, MAPK and PKC signaling cascades to phosphorylate Cx43 on serines 262, 279/282, and 368. Upon EGF treatment Cx43 phosphorylation transiently increased up to 4-fold and induced efficient (66.4%) GJ endocytosis as evidenced by a 5.9-fold increase in Cx43/clathrin co-precipitation.

1. Introduction

Direct intercellular communication by gap junction (GJ) channels is a hallmark of normal cell and tissue physiology. GJs are the only cell–cell junction type that allows direct cell–cell communication via the transfer of molecules between cells. Examples include small metabolites such as glucose, amino acids, and ATP; ions such as Na^+, Ca^{2+}, and Cl^-; cell signaling molecules such as IP3 and cAMP; and potentially functional RNAs, such as miRNAs in glioma cells [1] and siRNAs in NRK cells ([2], reviewed in [3]). Complete double-membrane spanning GJ channels are formed when two hexameric hemi-channels (connexons) dock in the extracellular space. In addition, based on their double-membrane configuration GJs likely contribute significantly to cell–cell adhesion. Clearly, these cellular GJ functions require precise modulation. Remarkably, docked GJ channels cannot be separated into individual hemi-channels under physiological conditions [4,5]. Yet, analyses in many different cell and tissue types revealed that cells endocytose their GJs constitutively, and efficiently after treatment with inflammatory mediators such as thrombin and endothelin, in response to treatment with the non-genomic carcinogen lindane, and under many physiological and pathological conditions that require cell–cell uncoupling and/or physical cell–cell separation such as cell migration in development and wound healing, tissue differentiation, mitosis, apoptosis, leukocyte extravasation, ischemia, hemorrhage, edema, and cancer cell metastasis [6–14]. Constitutive and acute GJ endocytosis correlates with the short half-life of 1–5 h reported for GJ proteins (connexins, Cxs) and GJs [7,15–17]. We have previously shown that GJs are endocytosed as a whole in a clathrin-mediated endocytic process [6,12,18,19]. However, the specific post-translational modifications such as phosphorylation, ubiquitination, etc. that may render Cx proteins in GJs endocytosis competent are still poorly understood.

Twenty Cx isoforms are found in mouse with Cx43 being the most prominent isoform. Cx43 is a well-known phospho-protein. Numerous serine residues in the Cx43 C-terminus are phosphorylated to up-regulate (Ser325, Ser328, Ser330, Ser364/365, and Ser373) or down-regulate (Ser255, Ser262, Ser279/282, and

Abbreviations: AGJ, annular gap junction; CME, clathrin mediated endocytosis; EGF, epidermal growth factor; GJ, gap junction; GJIC, gap junction intercellular communication; LY, lucifer yellow; MAPK, mitogen activated protein kinase; MEF, mouse embryonic fibroblast; mES cells, mouse embryonic stem cells; PKC, protein kinase C; PM, plasma membrane; RTK, receptor tyrosine kinase

* Corresponding author. Address: Department of Biological Sciences, Lehigh University, 111 Research Dr., Iacocca Hall, D-218, Bethlehem, PA 18015, USA. Fax: +1 610 758 4004.
E-mail address: MFalk@lehigh.edu (M.M. Falk).
[1] Current address: Department of Orthopaedic Surgery, Perelman School of Medicine, University of Pennsylvania, 3450 Hamilton Walk, 409 Stemmler Hall, Philadelphia, PA 19104, USA.

http://dx.doi.org/10.1016/j.febslet.2014.01.048
0014-5793/

Ser368) GJ mediated intercellular communication (GJIC) (reviewed in [20]). Protein kinase C (PKC) is thought to phosphorylate Cx43 at Ser368 to down-regulate GJIC [21,22]. Cx43 has also been shown to be a substrate of mitogen activated protein kinase (MAPK) that upon mitogen stimulation phosphorylates Cx43 at Ser255, Ser262, and Ser279/Ser282 to down-regulate GJIC [23,24]. Epidermal growth factor (EGF), a well-studied mitogen, binds to the EGF receptor (a receptor tyrosine kinase [RTK] family member) to activate both MAPK and PKC signaling pathways, to for example promote cell proliferation. Mouse embryonic stem (mES) cells are known to express the GJ proteins Cx31, Cx43, and Cx45 and to form functional GJs [25,26]. ES cells are actively proliferating cells with a relatively short cell cycle (see Supplemental Movie 1). They can infinitely self-renew while maintaining their pluripotency that is mediated via GJIC among the cells in the colony [27–29]. Treatment of mES cells with EGF is known to down-regulate GJIC [30]. However, the mechanism/s that lead to GJIC inhibition are not known. Since EGF can stimulate cell proliferation, and mitotic cells are known to remove their GJs at onset of mitosis [13], we hypothesized that EGF-treatment may lead to GJ endocytosis to down-regulate GJIC. To test this hypothesis, and to characterize signals that may lead to GJ endocytosis, we treated mES cell colonies with EGF. We found that EGF-treatment induced inhibition of GJIC that correlated with clathrin recruitment and Cx43–GJ endocytosis, and that GJ endocytosis was initiated by phosphorylation of Cx43 at serines 262, 279/282, and 368.

2. Materials and methods

2.1. Cell culture

E14TG2a mouse embryonic stem (mES) cells (ATCC, Cat. No. CRL-1821) were seeded on mouse embryonic fibroblasts (MEFs) (Millipore, Cat. No. PMEF-NL). Under established culture conditions described below mES cells remain undifferentiated and grow into 3-dimensional colonies that are only loosely attached to the culture dishes. Colonies were passaged and maintained in 0.1% gelatin-coated dishes (MEF-free) in humidified atmosphere containing 5% CO_2 at 37 °C in KO DMEM (Gibco, Cat. No. 10829). Media were supplemented for a final concentration of 15% with KO serum replacement (Gibco, Cat. No. 10828), 3 mM L-glutamine (Gibco, Cat. No. 25030), 50 I.U/ml penicillin and 50 μg/ml streptomycin (Gibco, Cat. No. 15070), 1 mM sodium pyruvate (Gibco, Cat. No. 11360, stock 100 mM), 1× non-essential amino acids (Millipore, Cat. No. TMS-001-C), 1× β-mercaptoethanol (Millipore, Cat. No. ES-007-E), and 1000 U/ml ESGRO mLIF (Millipore, Cat. No. ESG1106) to prevent cells from differentiating. Prior to EGF treatment (100 ng/ml EGF, Sigma, Cat. No. E4127), media were replaced with serum free media (to starve cells of growth factors) supplemented either with 50 μM PD98059 (MEK, MAPK pathway inhibitor; Sigma, Cat. No. P215), 100–500 nM chelerythrine-Cl (PKC inhibitor; Cayman Chemical, Cat. No. 11314), or both for 1 h and cultured under standard conditions.

2.2. Dye transfer assays

mES cell colonies were cultured in 3.5 cm diameter dishes for 2 days, then pre-incubated with serum free media as described above. Appropriate culture dishes were then treated with PD98059, chelerythine-Cl, or both and cultured for 1 h before adding 100 ng/ml EGF and incubating for additional 30 min. Media were replaced with 0.1% Lucifer Yellow (LY; Invitrogen, Cat. No. L682) in OPTIMEM (Gibco, Cat. No. 31985). To wound cells and allow for LY dye uptake, mES cell colonies were carefully cut with a sharp scalpel in the presence of LY, incubated at room temperature (RT) for 5 min to allow dye to transfer to neighboring cells, then washed 3 times with OPTIMEM followed by 3.7% paraformaldehyde fixation for 10 min. Paraformaldehyde was removed by washing 3 times with 1 × PBS containing Ca^{2+} and Mg^{2+}. LY fluorescence and Phase Contrast images were acquired using a 20× objective. Dye spreading from the injured cells to the farthermost receiving cells was measured using MetaVue software version 6.1r5 (Molecular Devices, Sunnyvale, CA), averaged and plotted. In addition, fluorescence intensities along lines placed perpendicular to the cut at representative areas were measured and plotted as well.

2.3. Immunofluorescence microscopy and image analyses

mES cell colonies were grown on glass cover slips pre-treated with 0.1% gelatin (Fisher Scientific, Cat. No. G-7) to improve colony adhesion; fixed and permeabilized in pure ice-cold ethanol for 10 min; blocked with 10% FBS in PBS at RT for 1 h, and incubated with primary rabbit polyclonal anti-Cx43 antibodies (Cell Signaling Technology, Cat. No. 3512) at 1:500 dilution at 4 °C overnight. Secondary antibodies (Alexa488-conjugated goat anti-rabbit, Molecular Probes/Invitrogen, Cat. No. A11008) were used at 1:500 dilution at RT for 1 h. Plasma membranes were visualized using 1 μg/ml Alexa594-conjugated wheat germ agglutinin (WGA; Molecular Probes/Invitrogen, Cat. No. W11262), or a monoclonal antibody directed against the membrane-associated protein, ZO-1 (at 1:300 dilution, Zymed Laboratories, Cat. No. 33-9100) combined with an Alexa568-conjugated secondary antibody (goat anti-mouse, at 1:500 dilution, Molecular Probes/Invitrogen, Cat. No. A-11031) after fixation in 3.7% formaldehyde and permeabilization in 0.2% Triton X-100. Cell nuclei were stained with 1 μg/ml DAPI. Cells were mounted using Fluoromount-G™ (SouthernBiotech, Cat. No. 0100-01) and examined. Wide-field fluorescence microscopy was performed on a Nikon Eclipse TE 2000E inverted fluorescence microscope equipped with a 40×, NA 1.4, Plan Apochromat oil immersion objective. Images were acquired using MetaVue software. Confocal microscopy was performed on a Zeiss Axiovert 200 M inverted fluorescence microscope equipped with an LSM510 META scan head and a 63×, NA 1.4, Plan Apochromat oil immersion objective. Argon-ion and Helium–Neon lasers were used to generate 488 and 543 nm excitation lines, and pinholes were typically set to 1 airy unit. Images were acquired and analyzed using ZEN software. Quantitative analyses were performed using ImageJ (National Institutes of Health, USA).

2.4. Electron microscopic analyses

mES cell colonies were cultured under feeder-free conditions in 3.5 cm diameter dishes, then fixed with 2.5% glutaraldehyde (Sigma, Cat. No. G7651) in 0.1 M sodium cacodylate buffer at RT for 2 h. Cells were washed, treated with tannic acid, dehydrated, uranyl acetate-stained and flat-embedded in the dishes as described in Falk [31]. Embedded cells were mounted, trimmed, thin-sectioned and examined with a Phillips CM100 electron microscope.

2.5. Western blot analyses

Denatured protein samples derived from mES cell lysates were analyzed on 10% SDS–PAGE mini-gels (BioRad). Biotinylated protein ladder (Cell Signaling Technology, Cat. No. 7727S) was used as a molecular weight marker. Proteins were transferred onto nitrocellulose membranes (Whatman, Cat. No. 10439396) on ice at 120 V for 1 h before blocking with 5% non-fat dry milk, or 5% BSA in TBST at RT for 1 h. Membranes were then incubated with primary antibodies at 4 °C overnight. Antibodies used were: rabbit anti-Cx43 (Cell Signaling Technology, Cat. No. 3512) at 1:2500 dilution, phospho-specific rabbit anti-Cx43 Ser255 (Santa Cruz,

Cat. No. sc-12899-R), phospho-specific rabbit anti-Cx43 Ser262 (Santa Cruz, Cat. No. sc-17219-R) both at 1:500, phospho-specific rabbit anti-Cx43 Ser279/282 [32] at 1:1000, phospho-specific rabbit anti-Cx43 Ser368 (Cell Signaling Technology, Cat. No. 3511) at 1:2000, phospho-ERK1/2 (Cell Signaling Technology, Cat. No. 9102) at 1:3000, mouse anti-clathrin heavy chain (BD Transduction Laboratories, Cat. No. 610499), at 1:2000, and mouse anti-α-tubulin (Sigma, Cat. No. T9026) at 1:5000 dilution. Membranes were washed with TBST followed by incubation with HRP-conjugated secondary antibodies (Zymed Laboratories, Cat. No. 81-6520 or 81-6120) at 1:10000 dilution at RT for 1 h. Proteins were detected with enhanced chemiluminescent (ECL) reagent. NIH ImageJ was used to quantify protein band intensities.

2.6. Co-Immunoprecipitation assays

mES cells were lysed with 1 × SDS-free RIPA buffer (Cell Signaling Technology, Cat. No. 9806) supplemented with protease and phosphatase inhibitor cocktail (Cell Signaling Technology, Cat. No. 5872). Supernatants were incubated with rabbit anti-Cx43 antibodies (Cell Signaling Technology) bound to protein-G magnetic beads (Dynabeads®, Invitrogen, Cat. No. 10003) at 4 °C overnight or RT for 2 h, then washed 3 times with 1 × TBS. Cx43 and bound proteins were eluted using hot SDS–PAGE sample buffer containing 50 mM DTT. Samples were analyzed by Western blot as described above.

2.7. Statistical analyses

Unpaired student *t*-tests were performed to analyze the distance of dye transfer (Fig. 1), and to calculate efficiency of EGF-mediated GJ endocytosis (Figs. 3A, S1) using GraphPad software (GraphPad Inc., La Jolla, CA). ANOVA with Dunnett's post hoc tests were used to compare the levels of serine phosphorylation in Cx43, and the amount of co-precipitated clathrin heavy chains (Figs. 2 and 4). Data are presented as mean ± S.E.M. In all analyses, a *P*-value $\leqslant 0.05$ (depicted with *, **, or ***) was considered statistically significant.

3. Results

3.1. EGF treatment inhibits GJIC in mES cell colonies by activating the MAPK signaling cascade

GJIC has been shown to play a crucial role in embryonic development, tissue function, and cellular homeostasis (reviewed in [26,33]). GJIC in pre-implantation mouse embryos as early as at the 8-cell stage was described by Lo and Gilula [14]. Cx protein expression and GJIC in mES cell colonies has also been described [25]. In 2008, inhibition of GJIC in mES cells treated with EGF has been described [30]. However, the mechanism/s that lead to GJIC-inhibition were not explored. Thus, to specifically examine the effects of EGF-treatment on Cx43, and to test whether specific Cx43 phosphorylation events may be responsible for the inhibition of GJIC and/or GJ endocytosis, we pre-incubated mES cell colonies either with or without PD98059 (a specific MEK inhibitor, an upstream kinase of the MAPK signaling cascade, see Fig. 5), chelerythrine-Cl (a PKC inhibitor), or both in serum free media before treating colonies with EGF. To assess GJIC inhibition, scrape loading/dye transfer assays using the GJ-permeable dye, Lucifer Yellow (LY) were performed, and GJIC-efficiency in EGF-treated cell colonies was compared to untreated cell colonies in 3 independent experiments. GJIC in EGF-treated cell colonies was significantly reduced to 36 ± 1.1% ($P = 0.0001$, $n = 41$) compared to untreated controls (100 ± 5.9%, $n = 35$) (Fig. 1A and B, columns 1, 2). Cell colonies pre-incubated in PD98059, or PD98059 and chelerythrine-Cl exhibited a similar level of GJIC comparable to untreated control cells (90 ± 2.5%, $P = 0.078$, $n = 59$ and 87 ± 6.1%, $P = 0.164$, $n = 19$, respectively), suggesting that the MEK inhibitor significantly abolished the GJIC inhibitory effect of EGF (Fig. 1A and B, columns 3, 5). Pre-treating cells with chelerythrine-Cl did only slightly reduce the inhibitory effect of EGF, resulting in a 49 ± 2.5% ($P = 0.0001$, $n = 11$) efficient GJIC (Fig. 1A and B, column 4). Together, these results indicate that EGF inhibits GJIC in mES cell colonies by activating the MAPK signaling cascade.

3.2. EGF activates MAPK and PKC in mES cell colonies to phosphorylate Cx43 on serines 262, 279/282, and 368

In order to examine which serine residues in the Cx43 sequence might be phosphorylated in response to EGF treatment, we implemented phospho-specific antibodies to detect the level of Cx43 phosphorylation at specific serine residues. mES cell colonies were cultured and serum-starved as described, then lysed at 10, 20, 30, 45, and 60 min post EGF treatment. Levels of phospho-Cx43 were analyzed by Western blots and intensities of protein bands were quantified. α-Tubulin levels were analyzed as a loading control. Results indicate that EGF induced Cx43 phosphorylation at specific serine residues located in its C-terminus. Levels of pSer262, pSer279/282, and pSer368 at 10, 20 and 30 min post EGF treatment were significantly higher than in the untreated control (Fig. 2A and B, red, green and purple columns). At later time points (45 and 60 min), serine phosphorylation levels again dropped to levels that were not significantly different from untreated controls. No significant increase in phospho-Ser255, another Cx43 MAPK site that is known to be phosphorylated in mitotic cells [34,35], was detected (see Section 4) (Fig. 2A and B, blue column).

3.3. EGF induces GJ endocytosis in mES cell colonies

We have previously demonstrated that cells utilize the clathrin-mediated endocytic (CME) machinery to endocytose GJs either constitutively or acutely after treatment with natural inflammatory mediators such as thrombin and endothelin [6,12,18,19]. GJ channel endocytosis at onset of mitosis in rat fibroblasts and NRK cells has also been described [13]. Thus, to examine whether EGF-induced Cx43 phosphorylation may also induce GJ internalization, mES cell colonies were treated with EGF and cultured together with appropriate untreated controls. Colonies were then fixed and stained with Cx43 specific antibodies, followed by Alexa488-conjugated secondary antibodies (Figs. 3A, S1, column 1). Plasma membranes (PMs) were visualized either by using Alexa594-conjugated wheat germ agglutinin (WGA) (Figs. 3A, S1, column 2), or antibodies specific for the protein ZO-1 followed by Alexa568-conjugated secondary antibodies (Fig. S1, column 2). When cell colonies were examined by wide-field fluorescence microscopy (Fig. 3A) or confocal microscopy (Fig. S1), an obvious increase in cytoplasmically located punctate Cx43 structures (presumably AGJ vesicles) was detected in EGF-treated cell colonies (Figs. 3A, S1, middle panels, labeled with arrowheads) when compared with untreated cells (Figs. 3A, S1, top panels). GJs appeared as puncta and short lines clearly located in the membranes between cells (Figs. 3A, S1, labeled with arrows). Note that ES cells only have small cytosolic volumes and hence AGJs often appear in close proximity to the PM. When GJs and AGJs were counted in 6 representative images, and ratios calculated and compared between treated and untreated cells, average GJ/AGJ ratios in untreated cells dropped from 68.8 ± 2.4% to 23.1 ± 8.0% in EGF-treated cells, representing a GJ endocytosis rate of 66.4% ($P = 0.0007$, $n = 68$ GJs and AGJs counted in total) in mES cell

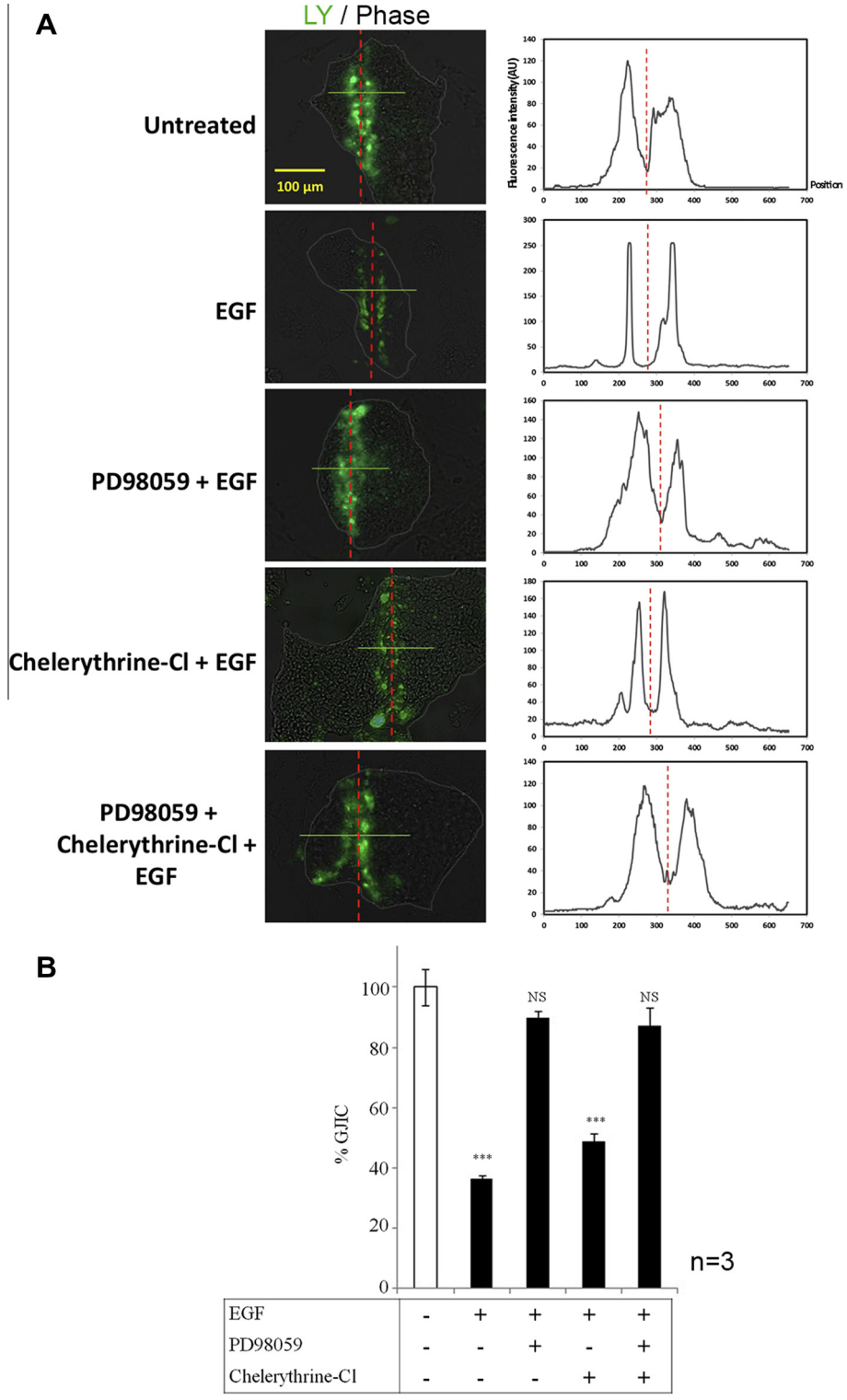

Fig. 1. EGF inhibits GJIC in mES cell colonies. mES cell colonies were treated with EGF in the presence or absence of the MEK-inhibitor PD98059 (MAPK signaling cascade), the PKC-inhibitor chelerythrine-Cl, or both followed by Lucifer yellow (LY) scrape loading dye transfer assays. Representative overlays of merged Phase Contrast and LY fluorescence images of 3 independent experiments are shown in (A), quantitative analyses of relative dye transfers (representative of GJIC efficiencies) are shown in (B). mES cell colonies are outlined by dotted lines. Scalpel-cuts through the colonies leading to cell wounding and dye-uptake are depicted by red lines. Fluorescence intensity profiles along lines (white) placed in representative areas perpendicular to the cuts are shown beside the images. In average, EGF-treatment reduced GJIC to 36%, while the MAP kinase cascade inhibitor, PD98059, counteracted the inhibitory EGF effect, and GJIC almost reverted to the level detected in untreated colonies (90%). Chelerythrine-Cl counteracted the inhibitory EGF effect only to some extent and GJIC efficiency remained low (49%). Addition of both inhibitors reverted GJIC to about the level observed for PD98059 alone, suggesting that the inhibitory EGF effect is mainly MAPK driven. NS = not significant.

colonies when treated with EGF. When colonies were pre-incubated with PD98059 prior to EGF-treatment, the average GJ/AGJ ratio was only slightly lower (63.3 ± 1.7%, $n = 60$ GJs and AGJs counted in 4 images) than the ratio observed in untreated cells correlating with the previously observed efficient inhibitory effect of PD98059 (Fig. 3A, bottom panel).

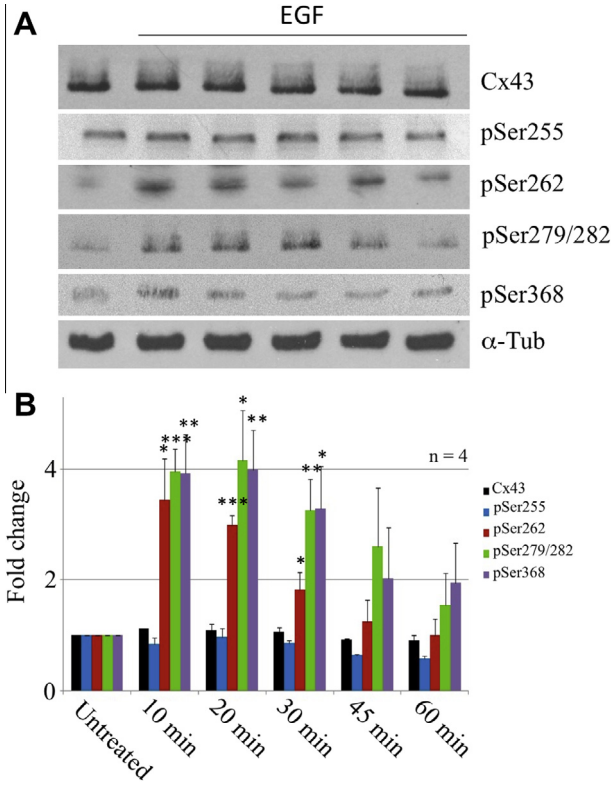

Fig. 2. EGF activates MAPK and PKC signaling cascades to phosphorylate Cx43 at serine residues 262, 279/282, and 368. mES cell colonies were treated with EGF before cell lysates were prepared at indicated times. Phosphorylated Cx43 was detected using phopho-specific antibodies directed against Ser255, Ser262, Ser279/282, and Ser368. Membranes were stripped and re-probed with anti α-Tubulin antibodies as a loading control. Representative blots are shown in (A), normalized quantitative analyses of phosphorylated Cx43 of 4 independent experiments are shown in (B). EGF induced a significant, 4-fold increase of Cx43 phosphorylation at serines 262, 279/282 (MAPK sites), and 368 (PKC site), but not on Ser255 (another MAPK site). Phosphorylation peaked between 10 and 30 min after EGF treatment.

To further support our conclusion that the cytoplasmic puncta represent internalized AGJ vesicles, we treated cells with EGF or PD98059 followed by EGF, and then performed EM analyses in comparison with untreated cells. Typical GJs were detected in the PMs between mES cell pairs in untreated and PD98059 plus EGF treated cells (Fig. 3B, left and right panels, marked with arrows). Consistent with our immunofluorescence data, we detected numerous AGJ vesicles in the cytoplasm of the EGF-treated cells (Fig. 3B, middle panels, marked with arrowheads). Note the typical, penta-laminar striped appearance of GJs and of the AGJ vesicle 'wall' that is representative of the double-membrane configuration of GJs. Also consistent, clearly less AGJs and more GJ plaques were detected in PD98059 plus EGF-treated cells (Fig. 3B, right panel). No AGJ vesicles were found in untreated cells. Taken together, our results suggest that EGF-treatment induces efficient GJ internalization in mES cells. Representative images from 6 independent immunofluorescence experiments and 2 independent EM studies are shown.

3.4. More clathrin is recruited to Cx43 GJs in EGF treated mES cell colonies

As described above, cells utilize the clathrin endocytic machinery to internalize their GJs [6,12,18,19]. Thus, the amount of clathrin that co-immunoprecipitates with Cx43 can be used as a direct measurement to quantify GJ endocytosis. We thus pre-treated mES cell colonies in serum free media for one hour with PD98059 (MEK inhibitor) and/or chelerythrine-Cl (PKC inhibitor), followed by treatment with EGF, and immunoprecipitation of Cx43 protein using magnetic beads. Mardin Darby canine kidney (MDCK) cells known not to express endogenous Cx43 protein [36], and untreated mES cell colonies were included as controls. Fractions of the cell lysates were collected for input analyses of Cx43 phosphorylation, ERK1/2 activity (=MAP kinase cascade activation), and protein loading (Fig. 4A). Consistent with the results shown in Fig. 2, Cx43 was substantially phosphorylated at Ser262, Ser279/282, and Ser368 after 30 min post EGF treatment (Fig. 4A, lanes 1, 2). Note, that the activity of ERK1/2, a late kinase of the MAPK signaling cascade (see Fig. 5), was significantly increased in EGF treated cells as indicated by the elevated levels of phosphorylated ERK1/2 that was detected with phospho-ERK-specific antibodies (Fig. 4A, row 5, lanes 2, 4). Also note that ERK1/2 activation/phosphorylation was effectively inhibited by PD98059, a specific inhibitor of the upstream MAP kinase MEK (Fig. 4A, row 5, lanes 3, 5). As a result and consistent with ERK1/2 inhibition, in PD98059 treated colonies, Cx43 phosphorylation at Ser262 and Ser279/282 (known Cx43 MAPK target sites [24]) was inhibited (Fig. 4A, rows 2, 3, lanes 3, 5). Likewise, in chelerythrine-Cl-treated colonies a significant reduction of EGF-induced Ser368 phosphorylation (a known Cx43 PKC target site [21]) was observed (Fig. 4A, row 4, lanes 4, 5).

Proteins that co-precipitated with Cx43 under these experimental conditions were analyzed by Western blot using antibodies specific for clathrin heavy chain (CHC) (Fig. 4B). The amount of CHC that co-immmunoprecipitated with Cx43 in EGF-treated mES cell colonies was increased in average by 5.9 ± 1.5-fold ($P < 0.01$, $n = 3$) when compared to untreated colonies (Fig. 4B, lanes 1, 2), strongly supporting our earlier finding that EGF induced GJ endocytosis. Only a somewhat increased (insignificant) clathrin co-precipitation was observed in cells that were pre-incubated with PD98059 (2.7 ± 0.9-fold; Fig. 4B, lane 3), or PD98059 and chelerythrine-Cl combined (2.8 ± 0.8-fold, Fig. 4B, lane 5), consistent with effective but incomplete blockage of respective kinase activity in these drug-treated cells. Interestingly, when cells were pre-incubated with chelerythrine-Cl alone followed by EGF treatment, still a significant 4.9 ± 1.3 ($P < 0.05$) fold increase in GJ internalization was observed (Fig. 4B, lane 4). Thus, chelerythrine-Cl did not significantly inhibit EGF-induced GJ endocytosis, suggesting that PKC-mediated phosphorylation of Ser368 is not sufficient to render Cx43-GJs internalization competent (see Section 4). No Cx43 or clathrin was immunoprecipitated in Cx43 negative MDCK control cells (Fig. 4A and B, lanes 6).

Taken together, our data (summarized in Fig. 5) suggest that EGF induces activation of the MAP kinase signaling cascade (including MEK and ERK1/2), and of PKC to phosphorylate Cx43 at Ser262, Ser279/282, and Ser368. These specific phosphorylation events render Cx43 protein subunits in GJs clathrin-binding capable to initiate the endocytosis of GJs in mES cells. Inhibiting MAPK activation by treating cells with the upstream MEK kinase specific inhibitor, PD98059, impedes Cx43 phosphorylation and in consequence, GJ internalization.

4. Discussion

EGF-mediated inhibition of GJIC in mES cell colonies has previously been observed by Park and colleagues [30]. However, no molecular mechanism/s explaining this observation have been reported. In WB-F344 and T51B rat liver epithelial cells, it was described that EGF-treatment induced inhibition of GJIC that was mediated by MAPK [23,37]. In principle, down-regulation of GJIC can be achieved by either GJ channel closure, and/or GJ endocytosis [38]. In 2004, by treating IAR20 rat liver epithelial cells in

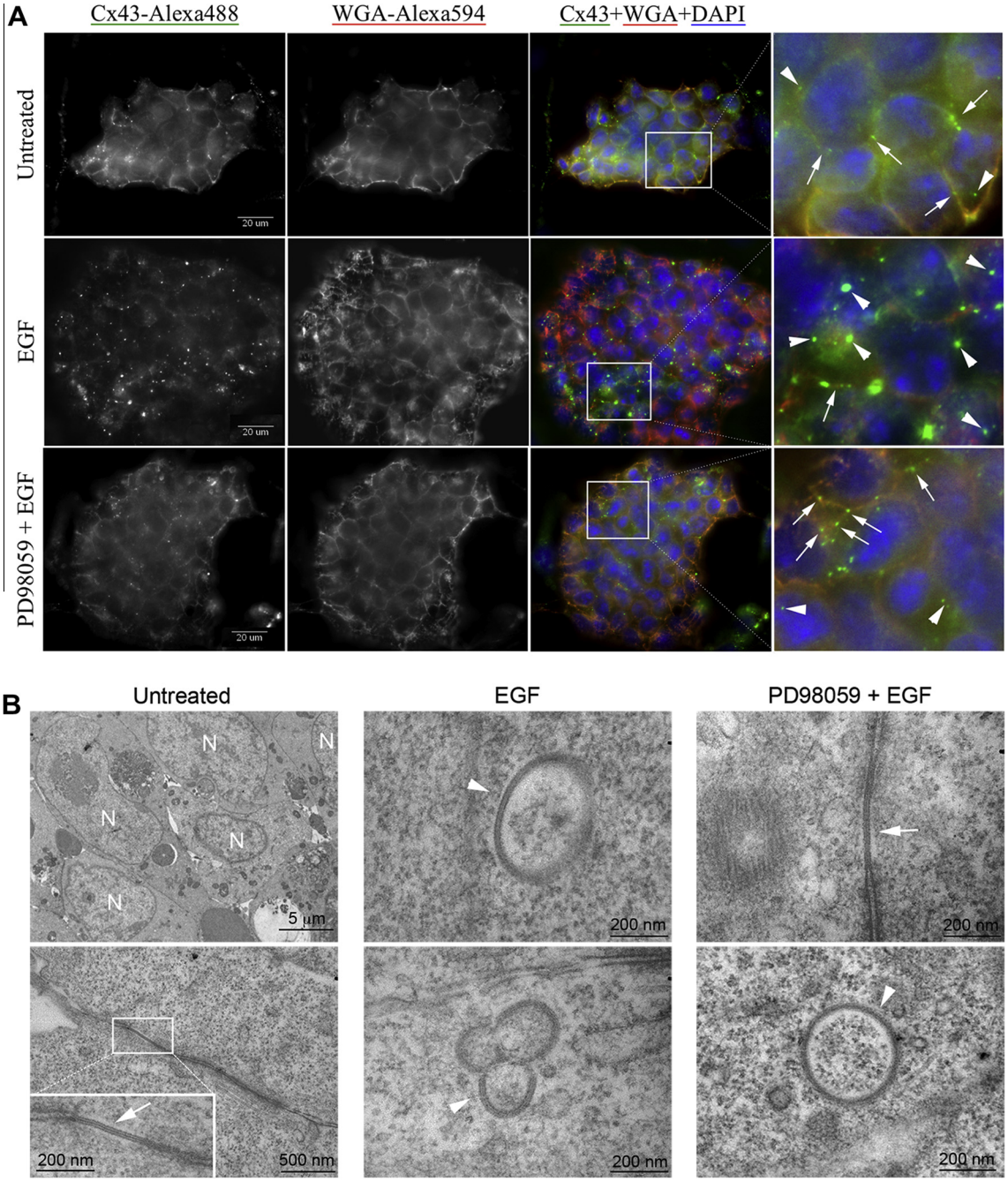

Fig. 3. EGF induces GJ endocytosis in mES cells. mES cell colonies grown on cover glasses were fixed and stained using antibodies specific for Cx43 (Alexa488-conjugated secondary antibodies, green). Alexa594-conjugated WGA (red) and DAPI (blue) were used to decorate PMs and label cell nuclei. (A) Representative wide-field immunofluorescence micrographs of 4 independent experiments are shown. Magnified views of boxed areas are shown on the right. An increased number of cytoplasmic Cx43 fluorescent puncta, indicative of internalized AGJ vesicles (labeled with arrowheads) were observed in EGF treated cells (middle panels). GJs, localized in the PM and appearing as puncta and short lines, are depicted by arrows. Noticeably less AGs are detected in untreated colonies (top panels), and in colonies that were treated with PD98059 plus EGF (bottom panels). Statistical analyses in EGF-treated and untreated colonies revealed an average GJ endocytosis efficiency of 66.4%. (B) Transmission electron micrographs revealed typically appearing, double-membrane (penta-laminar striped) GJs (marked with arrows) and AGJ vesicles (marked with arrowheads) in treated and untreated mES cell colonies, supporting the conclusion that cytoplasmic puncta detected in (A) probably are endocytosed GJs. A low-magnification overview image showing the densely arranged morphology of mES cells within a colony is shown in panel 1. N = cell nuclei.

hypertonic medium, Leithe and Rivedal gained initial evidence suggesting that the EGF-induced inhibition of GJIC was mediated by the internalization of Cx43-GJs, and that internalization may had been mediated by a clathrin-driven endocytic process [39]. However, again molecular signals that may be involved in this process have not been elucidated. In order to better understand the mechanism of EGF-induced GJIC-inhibition, we treated mES cell colonies with EGF, confirmed GJIC inhibition using dye-transfer assays (Fig. 1), examined whether EGF-treatment would lead to GJ endocytosis using imaging and clathrin-co-immunoprecipitation based assays (Figs. 3 and 4, S1), and analyzed whether potential concomitant phosphorylation events on specific serine residues located in the known regulatory Cx43 C-terminal domain would correspond to EGF treatment (Figs. 2 and 4). Implementing phospho-specific antibodies and kinase inhibitors, we uncovered that EGF-treatment induced specific Cx43 phosphorylation, and

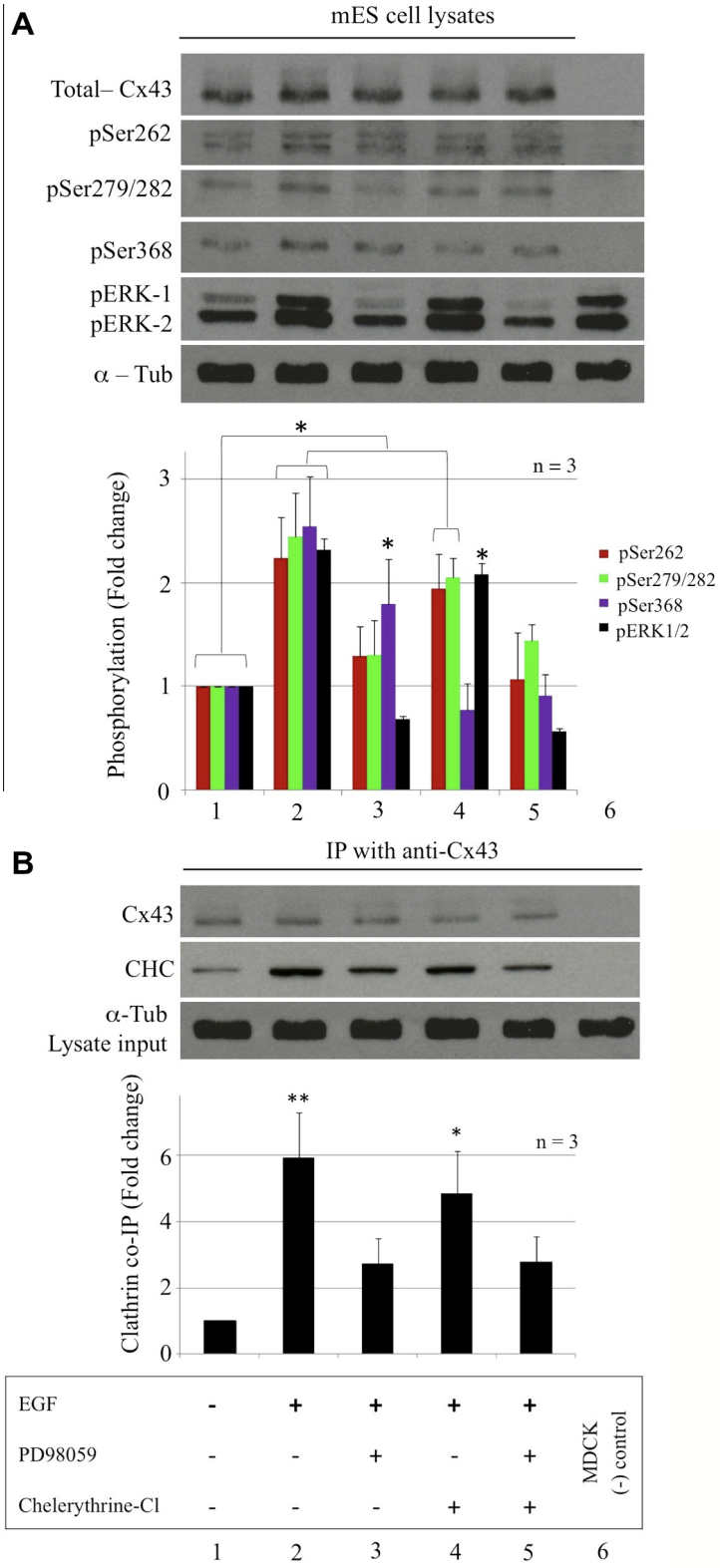

Fig. 4. Significantly increased amounts of clathrin, a direct indicator of GJ endocytosis, co-precipitates with Cx43 in EGF-treated mES cell colonies. (A) Western blot analyses of EGF-treated cell lysates show increased activity of ERK (as indicated by increased levels of phosphorylated ERK, pERK1/2), and increased phosphorylation of Cx43 at Ser262, Ser279/282, and Ser368 in cells treated for 30 min with EGF (lane 2) consistent with results shown in Fig. 2. Treatment with PD98059 (MEK/MAPK pathway inhibitor) plus EGF inhibited EGF-mediated phosphorylation of Ser262 and Ser279/282 (lanes 3, 5), while chelerythrine-Cl (PKC inhibitor) treatment inhibited EGF-mediated phosphorylation of Ser368 (lanes 4, 5). Untreated mES cells and non-Cx43 expressing MDCK cell lysates were analyzed in control (lanes 1, 6). (B) Cx43 polypeptides from lysates in (A) of 3 independent experiments were immunoprecipitated, and co-precipitated clathrin (CHC) was detected by Western blot analyses and quantified. Cx43 from EGF treated cells in average co-precipitated 5.9-fold more clathrin than in untreated control cells (lanes 1, 2). PD98059-treatment counteracted EGF-induced GJ internalization by inhibiting ERK1/2 (lanes 3, 5). Moderately increased levels of clathrin (4.9-fold) co-precipitated in cells treated with chelerythrine-Cl alone (lane 4). No Cx43 or CHC was precipitated in MDCK control cells.

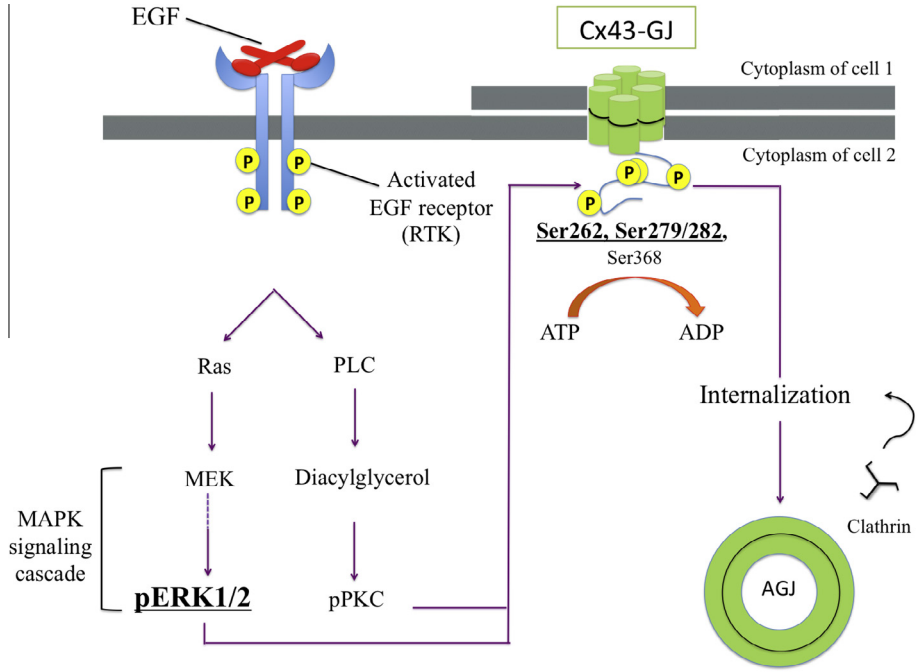

Fig. 5. Schematic representation illustrating EGF-induced, MAPK/PKC-mediated GJ internalization in mES cell colonies. EGF binds to phosphorylates and activates its receptor, a receptor tyrosine kinase (RTK) located in the PM of cells. Activated EGF-receptor activates MAPK and PKC signaling cascades to phosphorylate Cx43 at Ser262, Ser279/282, and Ser368. Phosphorylated Cx43 recruits clathrin and clathrin-adaptors to endocytose GJs.

that activation of ERK1/2 (MAPK signaling pathway) is responsible for EGF-mediated Cx43 phosphorylation at Ser262 and Ser279/282, whereas PKC activation is responsible for Ser368 phosphorylation (see Fig. 5). Recently, Johnson et al. reported that in pancreatic cancer cells mutation of serine residues 279 and 282 that prevented phosphorylation of these residues led to GJ internalization-deficiency [40]. Consistent with their findings, our data demonstrate that ERK1/2-mediated phosphorylation of Cx43 on Ser279/Ser282 also occurs upon EGF-treatment in mES cell colonies, and that this phosphorylation is required for GJ internalization in these cells.

Interestingly, we did not find a significant increase in Ser255 phosphorylation (another MAPK Cx43 target site) upon EGF-treatment of mES cell colonies (Figs. 2, 4A), as this was described to occur in 12-O-tetradecanoylphorbol 13-acetate (TPA)-treated epithelial IAR20 cells [35]. TPA is an analog of the second messenger, diacylglycerol (DAG) that is known to activate both, MAPK and PKC signaling pathways and to induce elevated phosphorylation and ubiquitination of Cx43 [35,41]. Observed differences might be explained by unalike experimental conditions (e.g. EGF versus TPA specificity) or they might be cell type specific (rat liver epithelial versus mES cells). In addition, besides its known cell-proliferative activity, EGF might have significant yet to be characterized additional effects on mES cells that require cellular uncoupling as well as GJ internalization (e.g. ES cell differentiation, migration, or channel-independent Cx43 signaling). Indeed, in recent years, the role of GJIC in mouse and human ES cell maintenance and differentiation, as well as its potential role in the reprogramming and differentiation of induced pluripotent stem (iPS) cells has attracted increasing attention. For example, it has been shown that GJIC is required for ES cells to maintain their pluripotent state [28]. In addition, Cx43 expression has recently been found to be important for the generation of iPS cells [27]. In 2008, Buehr et al. defined specific rat ES cell culture conditions that capture their authentic ES cell phenotype by using pharmacological inhibitors including MEK/ERK inhibitors [42]. Their findings together with our own results presented here indicate that ES cells utilize the EGF pathway, for example to regulate cell proliferation, differentiation as well as other essential events by modulating GJIC within the colonies. A clear understanding of the molecular mechanisms that lead to growth factor-induced inhibition of GJIC and GJ endocytosis are therefore of eminent importance.

We used PD98059, a MEK specific inhibitor, and monitored corresponding activation (phosphorylation) of ERK1/2 (upstream and downstream kinases of the MAPK signaling cascade, see Fig. 5) to inhibit EGF-induced GJIC. In addition, our results show that EGF-receptor activation in mES cell colonies also stimulates PKC to phosphorylate Cx43 on Ser368. However, inhibiting PKC-activation alone (by chelerythrine-Cl treatment) did not appear sufficient to inhibit EGF-induced GJ internalization, suggesting that activation of ERK1/2 (and the MAPK signaling cascade) may be more critical for EGF-induced GJ endocytosis than activation of PKC. Clearly, further studies will be required to fully understand a likely crosstalk between PKC and MAPK pathways in regulating GJIC and GJ internalization. Although the exact order of Cx43 phosphorylation events still needs to be determined, for the first time we provide compelling evidence that suggests that specific phosphorylation events renders Cx43 protein subunits in GJs clathrin-binding competent to induce GJ endocytosis.

Acknowledgements

We thank Dr. Paul Lampe (Fred Hutchinson Cancer Research Center, Seattle, WA) for his generous gift of pSer279/282 antibodies; Dr. Malcolm Wood (microscopy facility, The Scripps Research Institute, La Jolla, CA) for EM analyses; Tim Garelick (Department of Biological Sciences, Lehigh University, Bethlehem, PA) for his assistance in performing statistical analyses; and Falk lab members for constructive discussions and critical reading of the paper. These works were supported by NIHs NIGMS Grant GM55725-13 to M.M.F.

Appendix A. Supplementary data

Supplementary data associated with this article can be found, in the online version, at http://dx.doi.org/10.1016/j.febslet.2014.01.048.

References

[1] Katakowski, M., Buller, B., Wang, X., Rogers, T. and Chopp, M. (2010) Functional microRNA is transferred between glioma cells. Cancer Res. 70, 8259–8263.
[2] Valiunas, V. et al. (2005) Connexin-specific cell-to-cell transfer of short interfering RNA by gap junctions. J. Physiol. 568, 459–468.
[3] Brink, P.R., Valiunas, V., Gordon, C., Rosen, M.R. and Cohen, I.S. (2012) Can gap junctions deliver? Biochim. Biophys. Acta 1818, 2076–2081.
[4] Ghoshroy, S., Goodenough, D.A. and Sosinsky, G.E. (1995) Preparation, characterization, and structure of half gap junctional layers split with urea and EGTA. J. Membr. Biol. 146, 15–28.
[5] Goodenough, D.A. and Gilula, N.B. (1974) The splitting of hepatocyte gap junctions and zonulae occludentes with hypertonic disaccharides. J. Cell Biol. 61, 575–590.
[6] Baker, S.M., Kim, N., Gumpert, A.M., Segretain, D. and Falk, M.M. (2008) Acute internalization of gap junctions in vascular endothelial cells in response to inflammatory mediator-induced G-protein coupled receptor activation. FEBS Lett. 582, 4039–4046.
[7] Falk, M.M., Baker, S.M., Gumpert, A.M., Segretain, D. and Buckheit 3rd, R.W. (2009) Gap junction turnover is achieved by the internalization of small endocytic double-membrane vesicles. Mol. Biol. Cell 20, 3342–3352.
[8] Gilleron, J., Fiorini, C., Carette, D., Avondet, C., Falk, M.M., Segretain, D. and Pointis, G. (2008) Molecular reorganization of Cx43, Zo-1 and Src complexes during the endocytosis of gap junction plaques in response to a non-genomic carcinogen. J. Cell Sci. 121, 4069–4078.
[9] Ginzberg, R.D. and Gilula, N.B. (1979) Modulation of cell junctions during differentiation of the chicken otocyst sensory epithelium. Dev. Biol. 68, 110–129.
[10] Hesketh, G.G. et al. (2010) Ultrastructure and regulation of lateralized connexin43 in the failing heart. Circ. Res. 106, 1153–1163.
[11] Leach, D.H. and Oliphant, L.W. (1984) Degradation of annular gap junctions of the equine hoof wall. Acta Anat. (Basel) 120, 214–219.
[12] Piehl, M., Lehmann, C., Gumpert, A., Denizot, J.P., Segretain, D. and Falk, M.M. (2007) Internalization of large double-membrane intercellular vesicles by a clathrin-dependent endocytic process. Mol. Biol. Cell 18, 337–347.
[13] Boassa, D., Solan, J.L., Papas, A., Thornton, P., Lampe, P.D. and Sosinsky, G.E. (2010) Trafficking and recycling of the connexin43 gap junction protein during mitosis. Traffic 11, 1471–1486.
[14] Lo, C.W. and Gilula, N.B. (1979) Gap junctional communication in the preimplantation mouse embryo. Cell 18, 399–409.
[15] Beardslee, M.A., Laing, J.G., Beyer, E.C. and Saffitz, J.E. (1998) Rapid turnover of connexin43 in the adult rat heart. Circ. Res. 83, 629–635.
[16] Berthoud, V.M., Minogue, P.J., Laing, J.G. and Beyer, E.C. (2004) Pathways for degradation of connexins and gap junctions. Cardiovasc. Res. 62, 256–267.
[17] Fallon, R.F. and Goodenough, D.A. (1981) Five-hour half-life of mouse liver gap-junction protein. J. Cell Biol. 90, 521–526.
[18] Fong, J.T., Kells, R.M. and Falk, M.M. (2013) Two tyrosine-based sorting signals in the Cx43 C-terminus cooperate to mediate gap junction endocytosis. Mol. Biol. Cell 24, 2834–2848.
[19] Gumpert, A.M., Varco, J.S., Baker, S.M., Piehl, M. and Falk, M.M. (2008) Double-membrane gap junction internalization requires the clathrin-mediated endocytic machinery. FEBS Lett. 582, 2887–2892.
[20] Thevenin, A.F., Kowal, T.J., Fong, J.T., Kells, R.M., Fisher, C.G. and Falk, M.M. (2013) Proteins and mechanisms regulating gap-junction assembly, internalization, and degradation. Physiology (Bethesda) 28, 93–116.
[21] Lampe, P.D., TenBroek, E.M., Burt, J.M., Kurata, W.E., Johnson, R.G. and Lau, A.F. (2000) Phosphorylation of connexin43 on serine368 by protein kinase C regulates gap junctional communication. J. Cell Biol. 149, 1503–1512.
[22] Solan, J.L., Marquez-Rosado, L., Sorgen, P.L., Thornton, P.J., Gafken, P.R. and Lampe, P.D. (2007) Phosphorylation at S365 is a gatekeeper event that changes the structure of Cx43 and prevents down-regulation by PKC. J. Cell Biol. 179, 1301–1309.
[23] Kanemitsu, M.Y. and Lau, A.F. (1993) Epidermal growth factor stimulates the disruption of gap junctional communication and connexin43 phosphorylation independent of 12-0-tetradecanoylphorbol 13-acetate-sensitive protein kinase C: the possible involvement of mitogen-activated protein kinase. Mol. Biol. Cell 4, 837–848.
[24] Warn-Cramer, B.J., Lampe, P.D., Kurata, W.E., Kanemitsu, M.Y., Loo, L.W., Eckhart, W. and Lau, A.F. (1996) Characterization of the mitogen-activated protein kinase phosphorylation sites on the connexin-43 gap junction protein. J. Biol. Chem. 271, 3779–3786.
[25] Worsdorfer, P. et al. (2008) Connexin expression and functional analysis of gap junctional communication in mouse embryonic stem cells. Stem cells 26, 431–439.
[26] Wong, R.C., Pebay, A., Nguyen, L.T., Koh, K.L. and Pera, M.F. (2004) Presence of functional gap junctions in human embryonic stem cells. Stem cells 22, 883–889.
[27] Ke, Q. et al. (2013) Connexin 43 is involved in the generation of human induced pluripotent stem cells. Hum. Mol. Genet. 22, 2221–2233.
[28] Todorova, M.G., Soria, B. and Quesada, I. (2008) Gap junctional intercellular communication is required to maintain embryonic stem cells in a non-differentiated and proliferative state. J. Cell Physiol. 214, 354–362.
[29] Wong, R.C., Pera, M.F. and Pebay, A. (2008) Role of gap junctions in embryonic and somatic stem cells. Stem Cell Rev. 4, 283–292.
[30] Park, J.H., Lee, M.Y., Heo, J.S. and Han, H.J. (2008) A potential role of connexin 43 in epidermal growth factor-induced proliferation of mouse embryonic stem cells: involvement of Ca2+/PKC, p44/42 and p38 MAPKs pathways. Cell Prolif. 41, 786–802.
[31] Falk, M.M. (2000) Connexin-specific distribution within gap junctions revealed in living cells. J. Cell Sci. 113 (Pt 22), 4109–4120.
[32] Solan, J.L. and Lampe, P.D. (2007) Key connexin 43 phosphorylation events regulate the gap junction life cycle. J. Membr. Biol. 217, 35–41.
[33] Nagy, J.I., Dudek, F.E. and Rash, J.E. (2004) Update on connexins and gap junctions in neurons and glia in the mammalian nervous system. Brain Res. Brain Res. Rev. 47, 191–215.
[34] Lampe, P.D., Kurata, W.E., Warn-Cramer, B.J. and Lau, A.F. (1998) Formation of a distinct connexin43 phosphoisoform in mitotic cells is dependent upon p34cdc2 kinase. J. Cell Sci. 111 (Pt 6), 833–841.
[35] Sirnes, S., Kjenseth, A., Leithe, E. and Rivedal, E. (2009) Interplay between PKC and the MAP kinase pathway in Connexin43 phosphorylation and inhibition of gap junction intercellular communication. Biochem. Biophys. Res. Commun. 382, 41–45.
[36] Dukes, J.D., Whitley, P. and Chalmers, A.D. (2011) The MDCK variety pack: choosing the right strain. BMC Cell Biol. 12, 43.
[37] Abdelmohsen, K. et al. (2007) Epidermal growth factor- and stress-induced loss of gap junctional communication is mediated by ERK-1/ERK-2 but not ERK-5 in rat liver epithelial cells. Biochem. Biophys. Res. Commun. 364, 313–317.
[38] Spray, D.C. and Burt, J.M. (1990) Structure-activity relations of the cardiac gap junction channel. Am. J. Physiol. 258, C195–C205.
[39] Leithe, E. and Rivedal, E. (2004) Epidermal growth factor regulates ubiquitination, internalization and proteasome-dependent degradation of connexin43. J. Cell Sci. 117, 1211–1220.
[40] Johnson, K.E., Mitra, S., Katoch, P., Kelsey, L.S., Johnson, K.R. and Mehta, P.P. (2013) Phosphorylation on Ser-279 and Ser-282 of connexin43 regulates endocytosis and gap junction assembly in pancreatic cancer cells. Mol. Biol. Cell 24, 715–733.
[41] Fykerud, T.A. et al. (2012) Smad ubiquitination regulatory factor-2 controls gap junction intercellular communication by modulating endocytosis and degradation of connexin43. J. Cell Sci. 125, 3966–3976.
[42] Buehr, M. et al. (2008) Capture of authentic embryonic stem cells from rat blastocysts. Cell 135, 1287–1298.